Engineering Optical and Mirror Bi-stability Mechanically

Muhammad Junaid Khan

Department of Electronics

Quaid-i-Azam University, Islambad, Pakistan

A Thesis Submitted in Partial Fulfillment of the Requirements for the Degree of

Master of Philosophy in Electronics

September, 2023

DEPARTMENT OF ELECTRONICS
QUAID-I-AZAM UNIVERSITY
ISLAMBAD, PAKISTAN

A thesis entitled *Engineering Optical and Mirror Bi-stability Mechanically* by Muhammad Junaid Khan in partial fulfilment of the requirements for the degree of Master of Philosophy, has been approved and accepted by the following,

---

Supervisor
Dr. Farhan Saif (POP, S.I)
Professor
Department of Electronics
Quaid-i-Aazam University
Islamabad, Pakistan

Chairman
Dr. Qaiser Abbas Naqvi
Professor
Department of Electronics
Quaid-i-Aazam University
Islamabad, Pakistan

Acknowledgements

I take this graceful moment to thank the Almighty for his blessings which led me to write a manuscript like this. I am grateful to my Supervisor Dr. Farhan Saif who gave me an opportunity to work with him. I am really honoured to be his student. His guidance at each and every step helped me to accompalish my work. I could not finish this manuscript without his valuable suggestions and efforts. I also want to thank Dr. Hassan Mahmood who motivated me towards research. I appreciate my colleagues who lended their helping hands to solve the problems which I faced in my work. I am indebted to my parents for their support and sacrifice in making everything possible in my life. I want to thank all those friends and relatives who have directly or indirectly facilitated me to complete this thesis.

Muhammad Junaid Khan
September 01, 2023

Abstract

We demonstrate the occurrence of bistable behavior, both in terms of optics and mirror movement, within an externally modulated nano-transducer system. This setup comprises a Fabry-Perot cavity driven by a powerful laser and a weaker probe, generating opto-mechanical coupling. An electro-mechanical system introduces Coulomb coupling, introducing non-linearity that induces optical bistability in the average intracavity photon count, as well as mirror bistability in the steady mechanical motion of the mirrors.

Contents

List of Figures

Chapter 1

Introduction

The study scientific knowledge light, has been a cornerstone of physics since its inception. Light recognized as made of photons. It exhibits both classical and quantum phenomena. The interactions between light and matter at the smallest scale. [1–3] is topic interest. The momentum carried by electromagnetic field applies a force through radiation pressure, inducing movement in the cofining mirror of the cavity. This radiation pressure force leads to changes in the position of the movable mirror. Consequently, the optical path experiences a displacement, ultimately introducing non-linear characteristics to the system. This non-linear phenomenon gives rise to different non-classical aspects like optical bistability, resembling the non-linearity found in Kerr-medium situations[4–7].

The pressure force from the light affects both the optical and mechanical parts of a cavity resonator [8–10]. Such as transparency created by optomechanical effects and the process of Four-Wave Mixing. Researchers have formed hybrid quantum systems [11–13], by combining optomechanical resonators with different elements such as mechanical membranes [14–18], Bose-Einstein condensates or Fermions individual atoms with multiple energy levels, and combining opto-mechanical systems and electro-mechanical systems [19–21]. In these hybrid system, the special quantum traits of both mechanical and electronic parts become important. Wineland [22, 23] and his team were the first to notice these system, and then Zoller, Tian, Milburn, and colleagues developed the study terminology.

The optical cavity field acts in a non-linear way, creating optical bistability in the system. This results in a specific occurrence called hysteresis [24]. Researchers have studied the optical bistability that comes from the Kerr effect. They looked at this in a simple optomechanical system and also in mixed optomechanical systems containing trapped cold atoms [25–28] and two-level atoms[28]. Additionally, researchers have looked into this phenomenon in a mixed electro-optomechanical system where nanomechanical resonators[29] are connected.

Optical bistability could be useful in nonlinear quantum optics tasks like handling optical signals [30], creating optical switches [31], and making devices for optical communication[32][17, 33–37]. Combine an optomechanical system and an electromechanical system to create a small device that converts electrical and optical signals. The new nano system called nano-electro-optomechanical system (NEOMS) is created using two charged mechanical resonators named MR1 and MR2. The field of light inside the optical cavity is connected to MR1 by using a link that combines optics and mechanics.We apply two outside voltages, +V1 and -V2, to the mechanical resonators MR1 and MR2. This makes the resonators interact with each other through Coulomb coupling.We make the light inside the probe switch between two states and control the mirror's back-and-forth movement in the nano mirrors MR1 and MR2. We do this by changing the strength of signals that we apply only to the mechanical resonators.

Scientists have created a system where light and mechanics work together using things like two small spinning disks, a nano crystal beam, or a microwave with two small moving beams [38, 39]. We have used powerful mechanical forces to create devices that mix quantum spins photon devices [40] and vibrations, as well as to achieve very strong connections between exciton photon coupling [41] and vibrations. Scientists have studied a situation called optical bi-stability in different opto mechanical systems [26, 42–48] where light and mechanics interact. This happens because of a push from the light's pressure inside an optical cavity. We also introduce a controllable switch that works by controlling the two-state behavior under different test conditions.

We figure out the rules that control how the system works, including the

total Hamiltonian and Heisenberg Langevin equations that explain how things move, and then we find solutions where everything stays stable and consistent. We study how the number of photons inside the system's Intra cavity photon number between two states, with the help of two outside forces applied to the nano mechanical mirrors MR1 and MR2.we look at how the positions where the nano mechanical mirrors MR1 and MR2 can switch between two states when we use outside signals to change them.

Chapter 2

Nano-Opto-Electro-Mechanical Systems

The NOEMS main objective is to create innovative systems and devices with special characteristics and events that occur at the nanoscale. NOEMS has the potential to enable a wide range of applications like imaging, communication, sensing and computation, among others, by merging optical, electrical, and mechanical functions. Controlling the propagation of light is one of the most significant issues in optics and photonics, optical communications like modulation, optical switching, device and network reconfigurability in addition to imaging and sensing (such as beam steering). Nano-opto-electro-mechanical systems (NOEMS), In the field of nanophotonics considered one of the new platforms for researching mechanical and electrical freedoms, over the last few years, has seen rapid growth. Using the optical, mechanical and electronic degree of freedom in NOEMS offers exciting opportunities to handle information carriers, Here, it investigates the motion of light, flow of electrons, and mechanical vibration modes we see in both classical and quantum worlds.NOEMS concepts and technologies, high speed and low-power consumption switches, high-efficiency microwave-optical conversion devices, and multiple quantum information processing functions can be applied to its on-chip integration. The principles of NOEMS will introduce, the most recent advancements, important achievements[49, 50].

2.1 The Physical System

In 2015, Markus Aspelmeyer et al. Although optomechanical system exist in real world application. By using a simple one oscillator mirror in the Fabry-Perot cavity, it is most fundamental model connected two harmonic oscillators. In this section introduce its primary components the optical and mechanical resonator. The physical back ground of the optical and mechanical interaction[51].

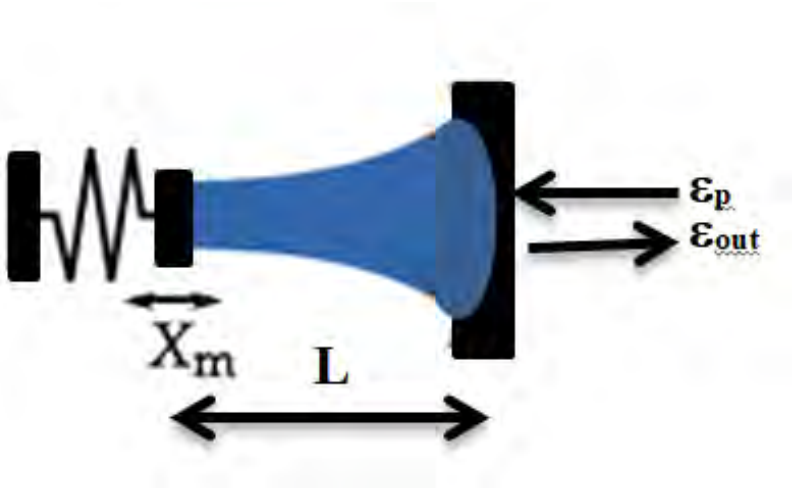

Figure 2.1: The optomechanical cavity length L is modulated by optical field, that causes a modulation of amplitude X_m. we express the incident optical field as ϵ_p, the output field $\epsilon_o ut$ and the length of the cavity as L.

2.2 The Mechanical Ocillator

It has been experimentally demonstrated that mechanical oscillators generally possess a large number of mechanical eigenmodes due to the high number of degrees of freedom and their size, whose geometry, material characteristics, and the coupling to its support are responsible for its spectral features. In general, a displacement field can be used to define the form of the spatial mechanical mode $u(r,t)$[52]. The $u(r,t)$ can be expanded interms of the oscillators eigen modes $u_n(r)$ and its related time-dependent amplitudes $X_n(t)$.

$$u(r,t) = \sum_n X_n(t) u_n(r), \tag{2.1}$$

Although the response of mechanical oscillators to applied forces is not linear but linearity offers a decent approximation for the tiny displacements and is often achievable in normal operation. The amplitude $X_n(t)$ is modeled with damped harmonic oscillation.

The damping component simultaneously serves as a temperature of the environment known as a "heat bath" and a source of noise for the mechanical oscillator, illustrates the coupling of the mechanical oscillator to its support.

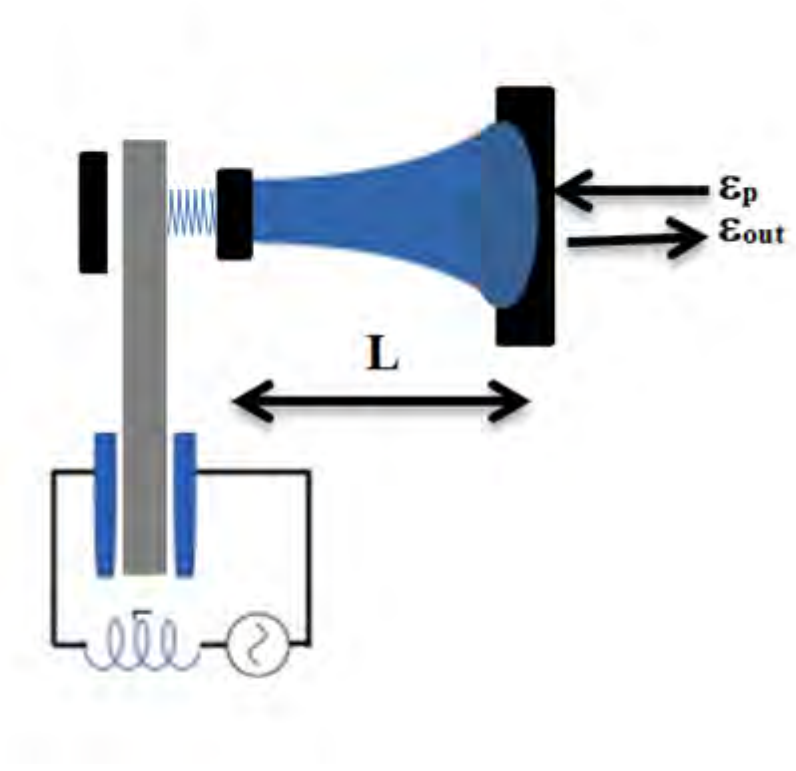

Figure 2.2: The schematics of an electromechanical setup. The capacitance $C(X_m)$ of the LC resonator is modulated by the mechanical motion.

The impact of the heat bath is modeled as a many harmonic oscillators in the group of infinitely in a thermal state at a temperature T. A Bose-Einstein distribution is followed by the mean bath occupation number and we have

$$n_B(\omega) = [e^{\hbar\omega/K_BT} - 1]^{-1}, \tag{2.2}$$

Here $\hbar$ and K_B represent the reduced Plank's constant and Boltzmann's constant respectively.

The mean bath occupancy at the mechanical frequency is

$$\bar{n} = n_B(\omega_m), \tag{2.3}$$

We can approximate $n_B(\omega_m)$ in the high-temperature limit with the help of the following relation

$$n_B(\omega) \approx \frac{K_BT}{\hbar\omega_m}, \tag{2.4}$$

The mechanical quality factor is defined as

$$Q_m = \frac{\omega_m}{\gamma_m}, \tag{2.5}$$

The quality factor and thermal decoherence rate are related as

$$\bar{n}\gamma_m \approx \frac{K_BT}{\hbar Q_m}, \tag{2.6}$$

To get minimal thermal decoherence, we require a high-Q mechanical oscillator and a low-temperature bath, which can be produced through cryogenic cooling of the experimental equipment.

For the quantum treatment of the mechanical oscillator we introduce position and momentum operators X_m, P_m, which fulfill canonical commutation relations $[X_m, P_m] = \imath\hbar$. We also introduce the dimensionless quadrature, as is typical in quantum optics $[x_m, p_m] = i$. They can also be defined in terms of creation and annihilation operators $c_m^\dagger$, c_m

$$[c_m, c_m^\dagger] = 1, \tag{2.7}$$

$$x_m = \frac{c_m + c_m^\dagger}{\sqrt{2}}, \tag{2.8}$$

$$p_m = \frac{c_m - c_m^\dagger}{\sqrt{2}\iota}, \tag{2.9}$$

By re-scaling with the ground state x_0 of the oscillator

$$X_m = \sqrt{2}x_0 x_m, \tag{2.10}$$

$$P_m = \sqrt{2}m_{eff}\omega_m x_0 p_m, \tag{2.11}$$

$$x_0 = \sqrt{\frac{\hbar}{2m_{eff}\omega_m}}. \tag{2.12}$$

2.3 The Optical Resonator

The second essential element in a cavity-optomechanical system is the optical cavity. This cavity acts as a container (Resonator) for photons that resonate within it. An example of such a cavity is the straightforward Fabry–Pérot cavity, which consists of two mirrors with high reflectivity placed L units apart. This arrangement results in a series of evenly spaced modes with distinct resonance frequencies, and the intervals between these frequencies are referred to as the free spectral range. The value of the free spectral range is defined by the length of the cavity no presence of an optical medium.

$$\nu_n = n\Delta\nu,\ \Delta\nu = \frac{c}{2L}, \tag{2.13}$$

In which a mechanical oscillator interact with a single cavity mode possessing a specific angular frequency denoted as $\omega_c = 2\pi\nu_c$. This particular configuration can be readily established through experimentation in setups involving nanoscale and microscale optomechanics. Consequently, interactions between distinct cavity modes are absent, as they do not couple with the mirror. However, it's worth noting that in certain systems, intentional or perturbative coupling can indeed take place between various optical modes.

$$F_{cav} = \frac{2\pi\Delta\nu}{\kappa} = \frac{\pi C}{\kappa L}, \tag{2.14}$$

Here κ represents the energy decaying rate that gives the number of photons in the cavity per unit time. Monitoring the output light of the cavity is a must for nearly every experiment if we are to distinguish between pure photon losses—absorption, scattering, and transmission into the external field—which we can finally quantify. Therefore, the overall decay rate is given by

$$\kappa = \kappa_{in} + \tilde{\kappa}, \tag{2.15}$$

where κ_{in} is the input-coupler of the cavity (i.e., the decay channel we can measure), and $\tilde{\kappa}$ is a collection of all other loss mechanisms that we are unable to detect. Assume a coherent laser field with a fixed center frequency of ω_0 and a complex amplitude ϵ that has been correctly re-scaled and is used to drive an optical cavity. This amplitude and the input power P_{in} are connected by

$$|\epsilon| = \sqrt{\frac{P_{in}}{\hbar\omega_0}}, \tag{2.16}$$

Here square root term describes the driving laser photon flux is considered. The equation of motion for the mean interactivity field α_c followed.

$$\dot{\alpha_c} = -(\imath\omega_c + \frac{\kappa}{2})\alpha_c + \sqrt{\kappa_{in}}\epsilon e^{-\imath\omega_0 t}, \tag{2.17}$$

At optical frequencies, we can get rid of the trivial evolution by introducing

$$\tilde{\alpha}_c(t) = \alpha_c(t)e^{\imath\omega_0 t}, \tag{2.18}$$

$\tilde{\alpha}_c$ will be assumed a constant steady state amplitude $\tilde{\alpha}_c^{ss}$ after a transient period.

$$\tilde{\alpha}_c^{ss} = \frac{\sqrt{\kappa_{in}}\epsilon}{\imath\Delta_0 - \frac{\kappa}{2}}, \tag{2.19}$$

with the de-tuning Δ_0 of the laser with respect to the cavity resonance frequency

$$\Delta_0 = \omega_0 - \omega_c, \tag{2.20}$$

We can distinguish between the input coupling rate κ_{in} and the overall decay rate κ, which causes a decrease in the interaction photon number with rising losses $\tilde{\kappa}$. We can obtain the linear response function for the cavity's susceptibility $\chi(\omega_0)$ by taking the Fourier transform of equation (2.33). The response of the system for a constant input at frequency ω_0 can be obtained with the value of $\chi(\omega_0)$ and is given by Lorentzian

$$\chi(\omega) = \frac{\sqrt{\kappa_{in}}}{\frac{\kappa}{2} - \imath(\omega - \omega_c)}, \tag{2.21}$$

The amplitude and phase responses of the intracavity field are given by its modulus and argument, respectively. The intracavity field in quantum mechanics can be expressed as a damped harmonic oscillator. To introduce the related dimensionless quadrature operators, the creation and annihilation operators $c_c^\dagger$, and c_c, respectively[53].

$$x_c = \frac{c_c + c_c^\dagger}{\sqrt{2}}, \tag{2.22}$$

$$p_c = \frac{c_c - c_c^\dagger}{\sqrt{2}\imath}, \tag{2.23}$$

x_c is referred to as the amplitude quadrature, and p_c is referred to as the phase quadrature of the electromagnetic field. the interaction between the optical and mechanical modes usually assumes the form of dispersive coupling. This implies that changes in the mechanical oscillator's position result in a shift in the cavity's resonance frequency. This interaction is physically mediated by radiation pressure, involving either momentum transfer through reflection (as seen in Fabry–Pérot setups and microtoroids) or gradient forces (as observed in setups with a membrane placed in the middle).

2.4 The Hamiltonian

A single mechanical mode interacts with a single optical mode. Expanding this concept to encompass scenarios with multiple modes is quite straightforward. The derivation of the Hamiltonian governing the interaction between a cavity and mechanical motion. Our starting point is the Hamiltonian that describes two harmonic oscillators operating independently without any coupling (uncoupled) between them.

$$H_0 = \hbar\omega_m C_m^\dagger C_m + \hbar\omega_c {C_c}^\dagger C_c, \tag{2.24}$$

The ω_m represents the resonance frequency of the mechanical motion, and ω_c stands for the resonance frequency of the optical cavity (also known as the nominal cavity frequency). We use $[c_i, c_j\dagger]$ to denote the commutation relation between operators c_i and $c_j\dagger$. The optical resonance frequency ω_c is determined by the time taken for photons to complete a round trip within the cavity. This, in turn, depends on the effective cavity length denoted as L. In other words, $\omega_c/2\pi = 2C/L$, where c is the speed of light. When the mirror undergoes displacement, it causes a shift in the resonance frequency. Consequently, this alteration impacts the energy contained within the cavity mode. Notably, for relatively small displacements $X_m/L << 1$, this effect becomes significant.

$$\omega_c(X_m) = \omega_c + \frac{\partial\omega_c}{\partial X_m} X_m + O(X_m)^2, \tag{2.25}$$

The Hamiltonian for the optomechanical system is considered. By taking into account first-order effects in X_m, the relationship $X_m X_0(C_m + C_m^\dagger) = \sqrt{2}X_0 X_m$ is utilized to derive the Hamiltonian that governs the optomechanical system.

$$H_{nl} = \hbar\omega_m C_m^\dagger C_m + \hbar\omega_c {C_c}^\dagger C_c + \hbar g_0 x_m C^\dagger C_c, \tag{2.26}$$

The single-photon optomechanical coupling strength.

$$g_0 = \sqrt{2}x_0\frac{\partial\omega_c}{\partial X_m}, \tag{2.27}$$

The connection between the mechanical oscillator and a single photon within the cavity is quantified by this equation. In the Fabry–Pérot scenario, $g_0 = \sqrt{2}X_0\omega_c/L$, and the inverse of L are relevant. It's noteworthy that, as per these definitions, a positive value for the displacement $X_m > 0$ results in an augmentation of cavity energy, signifying a reduction in the cavity length.

$$H_{drive} = -\imath\hbar[E^*(t)e^{\imath\omega_0 t}C_c - E(t)e^{-\imath\omega_0 t}C_c^\dagger], \tag{2.28}$$

The radiation-pressure interaction displays nonlinearity with respect to the amplitudes $c_i, c_i\dagger$, and it varies according to the photon number inside the cavity. However, due to the typically small value of g_0 in many current optomechanical systems, observing pronounced nonlinear dynamics and optomechanical effects at the single-photon level can be challenging. To amplify the influence of radiation pressure, one strategy involves employing a powerful laser beam to drive the optomechanical cavity. This laser beam carries a substantial coherent amplitude $\epsilon(t)$ that varies with time. Such a driving force, centered at the frequency w0, can be incorporated through the addition of an extra driving term.

$$H_{nl} = \frac{1}{2}\hbar\omega_m(x_m^2 + p_m^2) - \hbar\Delta_0 C_c^\dagger C_c + \hbar g_0 x_m C_c^\dagger C_c - \imath\hbar[E^*(t)C_c - E(t)C_c^\dagger], \tag{2.29}$$

For a strong laser drive the optomechanical Hamiltonian given in above equation (2.31) can be approximation.

$$H_{lin} = \hbar\omega_m C_m^\dagger C_m - \hbar\Delta_c {C_c}^\dagger C_c + \hbar\frac{g_0\alpha_c}{\sqrt{2}}(C_m + C^\dagger)(C_c + C^\dagger), \tag{2.30}$$

An effective detuning, Δ_c, has been introduced, which undergoes a shift from Δ_0 owing to the altered equilibrium position of the mirror. The coupling strength $g = g_0\alpha_c/\sqrt{2}$ of the linear interaction is enhanced by the inclusion of

the term α_c. In the current context, α_c denotes the square root of the photon number within the cavity. When a high-finesse cavity or a robust laser drive is dealt with, a considerable average photon count within the cavity can be observed. Consequently, the strength of interaction can undergo a significant increase by several orders of magnitude.

$$H_{bs} = \hbar g(C_m C_c^\dagger + C_m C_c), \tag{2.31}$$

The detuning, Δ_c, allows us to recognize various interaction modes arising from the linearized radiation pressure Hamiltonian. One such interaction mode is referred to as the beam-splitter (BS) Hamiltonian.

$$H_{tms} = \hbar g(C_m C_c + C_m^\dagger C_c^\dagger), \tag{2.32}$$

The above equation becomes resonant when $\Delta_c = -\omega_m$ is matched, The coherent transfer of energy between the mechanical oscillator and the cavity mode is observed. This aspect cooling down the mechanical motion using sideband cooling techniques and can also be harnessed to achieve a state exchange between the two modes. This specific interaction is known as the two-mode squeezing (TMS) interaction.

2.5 Quantum Langevin Equations

1. Heisenberg Uncertainty Principle:
The Heisenberg uncertainty principle is a fundamental concept in quantum mechanics that states that certain pairs of physical properties, such as position and momentum, cannot be precisely measured simultaneously. The more accurately you measure one property, the less accurately you can measure the other. This intrinsic uncertainty is a fundamental aspect of quantum mechanics.

2. Langevin Equation:
The Langevin equation is a stochastic differential equation commonly used to describe the motion of particles in a fluctuating environment. It accounts for both deterministic forces (such as applied forces) and random forces (representing the influence of the surrounding environment). The Langevin equation is often used in classical mechanics to model the behavior of particles undergoing Brownian motion.

3. Heisenberg-Langevin Approach:
The Heisenberg-Langevin approach extends the ideas of the Langevin equation to the context of quantum mechanics. It considers the effects of noise and fluctuations on quantum observables, similar to how the Langevin equation describes the motion of classical particles in a noisy environment.

The Heisenberg-Langevin approach is particularly useful for understanding how quantum systems respond to external influences and fluctuations. It is often applied in fields such as quantum optics, quantum electronics, and quantum information theory, where quantum systems are frequently subjected to environmental noise that can affect their behavior.

2.6 Quantum Fluctuations and Noise in the Heisenberg Langevin Framework

The optical cavity experiences a strong laser field with frequency ω_l and a probe field with frequency ω_p. Furthermore, the mechanical resonators MR_1

and MR_2 are subjected to external driving fields with amplitudes and correspondingly.

Δ_c : This term likely represents a frequency detuning of the system.

κ : This is a decay rate parameter that represents the rate at which the quantum system loses energy or information.

G_0 : This parameter might represent an optomechanical coupling constant related to the interaction between different parts of the system. It can affect the dynamics of the system.

$b_1^\dagger$ and b_1 : These are likely operators related to the creation and annihilation of particles in a quantum system, specifically the quantum field

$\sqrt{2\kappa}C_{in}(t)$: This term involves an input quantum field $C_{in}(t)$ and accounts for the interaction of the system with an external environment. The term $\sqrt{2\kappa}$ is likely relates to the strength of the interaction.

$$\dot{c} = -(\iota\Delta_c + \frac{\kappa}{2})c + \iota G_0(b_1^\dagger + b_1)c + \epsilon_l + \epsilon_p e^{-\iota\delta t} + \sqrt{2\kappa}c_{in}(t), \tag{2.33}$$

ω_1 : This term likely represents the oscillation frequency of a MR1.

ω_2 : This term likely represents the oscillation frequency of a MR2.

ϵ_1 : The external modulating fields ϵ_1 associated with MR1.

ϵ_2 : The external modulating fields ϵ_1 associated with MR2.

γ_1 : This is a decay rate parameter that represents the rate at which energy or information is lost from b_1

γ_2 : This is a decay rate parameter that represents the rate at which energy or information is lost from b_2

$\sqrt{2\kappa}\zeta_1$: This term involves a stochastic process or the Brownain noise operators $\zeta_1(t)$ with an external environment. The term $\sqrt{2\kappa}$ is likely related to the strength of the interaction.

$\sqrt{2\gamma_2}\zeta_2$: This term involves a stochastic processor or Brownain noise operator $\zeta_2(t)$ and accounts for the interaction of with an external environment. The term $\sqrt{2\gamma_2}$ likely relates to the strength of the interaction.

$$\dot{b}_1 = -(\iota\omega_1 + \frac{\gamma_1}{2})b_1 + \iota G_0 c^\dagger c - \iota G_c b_2 + \epsilon_1 e^{-\iota\delta t - \iota\phi_1} + \sqrt{2\kappa}\xi_1(t), \tag{2.34}$$

$$\dot{b}_2 = -(\iota\omega_2 + \frac{\gamma_2}{2})b_2 - \iota G_c b_1 + \epsilon_2 e^{-\iota\delta t - \iota\phi_2} + \sqrt{2\gamma_2}\xi_2(t), \tag{2.35}$$

$\hat{c}_{in}$ signifies the input vacuum noise linked to the cavity field, featuring a zero mean value. Meanwhile, the expressions ζ_1(t) and ζ_2(t) stand for Brownian noise operators related to the damping of MR1 and MR2 respectively. The symbols κ and γ_i (i = 1, 2) represent decay terms connected to the cavity and MRi (i = 1, 2) correspondingly. Employing the mean field approximation, the noise term mean values are averaged to zero, considering dissipation and fluctuation components. This process leads us to the equations.

8

$$\langle\dot{c}\rangle = -(\iota\Delta_c + \frac{\kappa}{2})\langle c\rangle + \iota G_0(\langle b_1^\dagger\rangle + \langle b_1\rangle)\langle c\rangle + \epsilon_l + \epsilon_p e^{-\iota\delta t} + \sqrt{2\kappa}c_{in}(t), \tag{2.36}$$

$$\langle\dot{b}_1\rangle = -(\iota\omega_1 + \frac{\gamma_1}{2})\langle b_1\rangle + \iota G_0\langle c^\dagger\rangle\langle c\rangle - \iota G_c\langle b\rangle_2 + \epsilon_1 e^{-\iota\delta t - \iota\phi_1} + \sqrt{2\kappa}\xi_1(t), \tag{2.37}$$

$$\langle\dot{b}_2\rangle = -(\iota\omega_2 + \frac{\gamma_2}{2})\langle b_2\rangle - \iota G_c\langle b_1\rangle + \epsilon_2 e^{-\iota\delta t - \iota\phi_2} + \sqrt{2\gamma_2}\xi_2(t), \tag{2.38}$$

With these three equations we obtain the steady-state solutions.we see the effective detuning is $\Delta = \Delta_c - G_0 q_{1s}$, Also $\wp_p \ll \wp_l$, , only consider strong laser power

$$c_s = \frac{\epsilon_l + \epsilon_p}{\iota\Delta + \frac{\kappa}{2}}, \tag{2.39}$$

$$b_{1s} = \frac{\iota G_0|c_s|^2 - \iota G_c b_{2s} + \epsilon_1 e^{-\iota\phi_1}}{\iota\omega_1 + \frac{\gamma_1}{2}}, \tag{2.40}$$

$$b_{2s} = \frac{-\iota G_c b_{1s} + \epsilon_2 e^{-\iota\phi_2}}{\iota\omega_2 + \frac{\gamma_2}{2}}. \tag{2.41}$$

Chapter 3

The Model

We consider a high-Q Fabry-Perot cavity of length L. According to Figure 1, the cavity is made up of a fixed mirror and a movable nano-mechanical resonator MR1, with a driving field and a probe field, as shown in Fig. 4.1 The total Hamiltonian of the given system is

The equation you've provided represents the total Hamiltonian $\hat{H}$ of a physical system as the sum of three distinct components: $\hat{H}_{mc}$ $\hat{H}_{dr}$ and $\hat{H}_{int}$ In quantum mechanics, the Hamiltonian operator represents the total energy of a system and governs its time evolution. Let's see the equation and its components:

3.1 Total Hamiltonian of the System

We examine a high-Q Fabry-Perot cavity characterized by its length, denoted as L. This cavity comprises a stationary mirror MR_{fixed} and a movable nano-mechanical resonator MR_1, subject to a driving field ϵ_l and a probe field ϵ_p. External modulating fields drive mirrors MR_1 and MR_2 individually. Furthermore, MR_1 is linked to the cavity field through the radiation pressure force, and it connects to another movable mirror MR_2 via an adjustable electrostatic Coulomb coupling force. The oscillation frequency of MR_1 is ω_1, and that of MR_2 is ω_2. The strength of Coulomb coupling is regulated through bias voltages: $+V_1$ for MR_1 and $-V_2$ for MR_2. This implies that, alongside the opto-mechanical coupling, the system includes a modifiable Coulomb coupling in-

tensity.

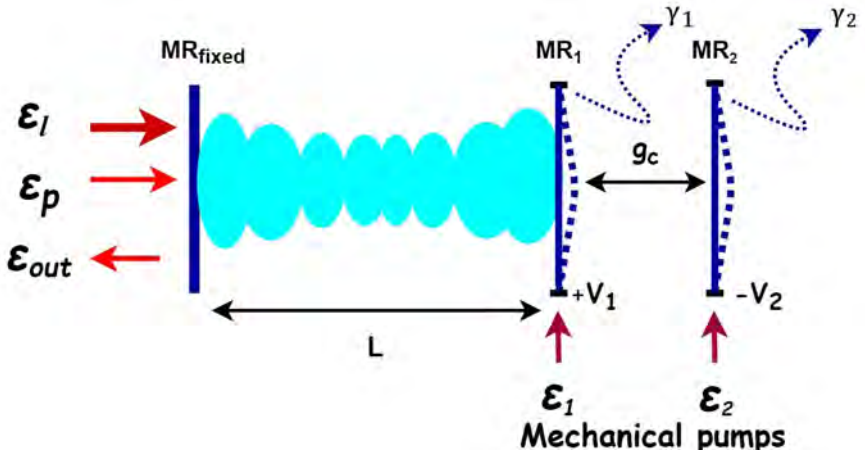

Figure 3.1: The schematic of the Nano-Electro-Opto-Mechanical system.The mechanical resonator MR_1 is connected to the cavity field via optomechanical coupling represented by g_0, and the second mechanical resonator MR_2 through the strength of Coulomb coupling, g_c. An input laser field with amplitude ϵ_l and a probe field with amplitude ϵ_p are introduced into the cavity through the fixed mirror. Furthermore, MR_1 is influenced by the biased voltage $+V_1$, while MR_2 is influenced by the biased voltage $-V_2$. In this context, L signifies the cavity's length, ϵ_1 and ϵ_2 refer to the external driving fields on MR_1 and MR_2 respectively, ϵ_{out} pertains to the output probe field, and γ_1 and γ_2 denote the mirror decay rates.

$$\hat{H} = \hat{H}_{mc} + \hat{H}_{dr} + \hat{H}_{int}. \tag{3.1}$$

3.2 Mirror and Field Hamiltonian

In the uncoupled scenario, denoted by H_{mc}, within a rotating reference frame at frequency, the mirror and field Hamiltonian is observed. The detuning of the cavity field frequency is indicated by $\Delta_c = \omega_c - \omega_l$. The initial component embodies the single-mode of the cavity field, characterized by frequency ω_c and the annihilation (or creation) operator $\hat{c}(\hat{c}^\dagger)$. The following two terms correspond to the independent Hamiltonian of the movable mirrors, MR_i, each having mass m_i and oscillating at frequency ω_i, where i = 1; 2. The operators,

q_i, and p_i, symbolize position and momentum, respectively.

$$\hat{H}_{mc} = \hbar\Delta_c \hat{c}^\dagger \hat{c} + \left[\frac{\hat{p}_1^2}{2m_1} + \frac{1}{2}m_1\omega_1^2\hat{q}_1^2\right] + \left[\frac{\hat{p}_2^2}{2m_2} + \frac{1}{2}m_1\omega_2^2\hat{q}_2^2\right]. \tag{3.2}$$

3.3 Driving Field Hamiltonian

$\hat{H}_{dr}$ combine Hamiltonian of various components, including the strong laser field with amplitude ϵ_l, the weak probe field with amplitude ϵ_p and the external driving fields ϵ_1 and ϵ_2. Here, $\delta_c = \omega_p - \omega_l$ symbolizes the detuning frequency of the probe field from the laser frequency ω_l. The initial two terms represent the classical light fields (pump and probe) at frequencies ω_l and ω_p respectively. The strong laser power $\wp_l$ and the probe field power $\wp_l$ correspond to ω_l and ω_p through relations ϵ_l and ϵ_p, respectively. The ultimate term depicts the Hamiltonian of external modulation applied to MR1 and MR2, where ϵ_j (j = 1; 2) denotes amplitude and phase. The symbols b_j and $b_j\dagger$ correspond to the phonon annihilation and creation operators of MR1 and MR2 respectively. Minor oscillations of the MRs from their mean positions can be defined as $qj = \sqrt{\frac{\hbar}{2m_j\omega_j}}(b_j + b_j\dagger)$. Similarly, the oscillations in mirror momenta can be described using the relation $\dot{q}_j = p_j/m_j$. The third Hamiltonian term, Hint, represents the coupling between the cavity field and MR1 through opto-mechanics, along with the Coulomb coupling linking MR1 and MR2. This is expressed as:

$$\hat{H}_{dr} = \iota\hbar\epsilon_l(\hat{c}^\dagger - \hat{c}) + \iota\hbar\left(\epsilon_p e^{-\iota\delta t}\hat{c}^\dagger - \epsilon_p^* e^{\iota\delta t}\hat{c}\right) + \iota\hbar\left[\Sigma_{j=1}^2\left(\epsilon_j\hat{q}_j e^{-\iota\delta t+\iota\Phi_j} - \epsilon_j\hat{q}_j^\dagger e^{-\iota\delta t-\iota\phi_j}\right)\right]. \tag{3.3}$$

3.4 Interaction Hamiltonian

The component signifies the interaction between MR1 and the cavity field due to opto-mechanical coupling. The following element represents the Coulomb-based coupling involving the moving mirrors. Specifically, the optomechanical

coupling strength, denoted as $g_0 = (\frac{\omega_c}{L}\sqrt{\frac{\hbar}{2m_1\omega_1}})$, is calculated as g0 = wc, while the Coulomb coupling strength is represented as $g_c = \frac{\kappa_c C_1 V_1 C_2 V_2}{\hbar r_0^3}$. The stable distance between the two resonators is denoted as r0. In terms of phonon annihilation (or creation) operators, it can be expressed as $b_j(b_j^\dagger)$.

$$\hat{H}_{mc} = -\hbar\Delta\hat{c}^\dagger\hat{c} + \hbar\omega_1 b_1^\dagger b_1 + \hbar\omega_2 b_2^\dagger b_2. \tag{3.4}$$

$$\hat{H}_{int} = -\hbar g_0 \hat{c}^\dagger\hat{c}\hat{q}_1 + \hbar g_c \hat{q}_1\hat{q}_2, \tag{3.5}$$

The detuning frequency of the probe field from the laser frequency is denoted as $\delta_c = \omega_p - \omega_l$. The initial two terms encompass the classical optical fields (pump and probe) characterized by frequencies ω_1 and ω_2 respectively. The relationship between the strong laser power $\wp_l$ and the probe field power is expressed through the variables $\epsilon_l = \sqrt{\frac{2\kappa\wp_l}{\hbar\omega_l}}$ and $\epsilon_p = \sqrt{\frac{2\kappa\wp_l}{\hbar\omega_p}}$ respectively.

$$\hat{H}_{int} = -\hbar G_0 \hat{c}^\dagger\hat{c}(b_1 + b_1^\dagger) + \hbar G_c(b_1^\dagger b_2 + b_1 b_2^\dagger). \tag{3.6}$$

The $G_0 = g_0\sqrt{\frac{\hbar}{2m_1\omega_1}}$ and $G_0 = g_c\sqrt{\frac{1}{2m_1 m_2\omega_1\omega_2}}$

Chapter 4

Optical Bi- Stability Results

The optical bistability has been observed experimentally in micro cavities[48]. In our work the bistability behaviour is the effect of non linearity that comes from the strength of optomechanical coupling G_0 and the strength of coulomb coupling G_c. The solution of equation (3.6) provides us with steady state values of cavity photon number and is given below

$$|\epsilon_l + \epsilon_p|^2 = |c_s|^2 \left[\frac{\kappa^2}{4} + (\Delta_c - G_0(b_{1s}^* + b_{1s}))^2 \right]. \tag{4.1}$$

Here $|c_s|^2 = c_s c_s^*$.The occurrence of bistable behavior in the system can be seen through this equation. In equation (3.8), if we take $G_0 = 0$ then the bistabillity in photon number will vanishes. We can obtain a third order polynomial of the steady state intracavity photon numbers by rearranging the equation (3.8) as below

$$a_1 x^3 + a_2 x^2 + a_3 x + a_4 = 0. \tag{4.2}$$

Where

$$x = |c_s|^2. \tag{4.3}$$

$$a_1 = G_0^2 a_1^2, \tag{4.4}$$

$$a_2 = 2\alpha_1(\Gamma + \Delta_c G_0), \tag{4.5}$$

$$a_3 = \left(\frac{\kappa^2}{4} + \Delta_c^2 + G_0\Gamma(G_0\Gamma + 2\Delta_c)\right), \tag{4.6}$$

$$a_4 = -|\epsilon_l + \epsilon_p|^2, \tag{4.7}$$

Here, $\alpha_1 = \beta_1 + \beta_1^*$, $\Gamma = \alpha_2\epsilon_2 + \alpha_3\epsilon_1$, $\alpha_2 = \beta_2 e^{-\iota\phi_2} + \beta_2^* e^{\iota\phi_2}$, $\alpha_3 = \beta_3 e^{\iota\phi_1} + \beta_3^* e^{\iota\phi_1}$, $\beta_1 = \frac{\iota(\iota\omega_2+\gamma_2/2)G_0}{(\iota\omega_1+\gamma_1/2)(\iota\omega_2/2)+G_c^2}$, $\beta_2 = -\frac{G_c}{G_0}\frac{\beta_1}{(\iota\omega_2+\gamma_2/2)}$ *and* $\beta_3 = \frac{-\iota\beta_1}{G_0}$. This equation has three roots, two of which correspond to stable regimes of the steady state photon number and the third to an unstable regime. with inflection and critical points, i.e. $y_c = \frac{-b\pm\sqrt{b^2-3ac}}{3a}$ and $y_{inf} = -b/3a$. The solutions of the cubic polynomial equation $ay^3 + by^2 + cy + d = 0$ provides the branches of the bi-stable curve. Using the solutions for y_c and y_{inf} , we can write the critical and inflection points of the Equation (5.1) as,

$$x_{c\pm} = \frac{-a_2/a_1 \pm \sqrt{(a_2/a_1)^2 - 3a_3/a_1}}{3}, \quad x_{inf} = -a_2/3a_1, \tag{4.8}$$

where x_{c+} and x_{c-} are critical points of upper and lower stable limbs of the bistable curve respectively, while x_{inf} is the inflection point of the curve. The range of the bistability window is determined by these critical points and at these points the driving laser field power $\wp_l$, has a corresponding window also. We think our new system works with small differences between vibration frequencies, and these small differences can change when the laser light is stronger. So, when we make the laser light stronger, the number of photons also goes up. So, when the laser is really strong within a specific range, the number of photons stays in two different states. When we make the laser even stronger, the light's change in frequency comes close to a specific value, which we call "critical detuning." At this critical point, the two states of photon number start to appear. This special frequency value decides when the two states happen in the system.

$$\Delta_c = \sqrt{3}\kappa \tag{4.9}$$

We want to explore how to control when light and mirrors switch between two states in the new nanosystem we made (NEOMS). We use some numbers from recent experiments [31, 32]. The cavity inside NEOMS has a length of $L = 25\,\text{cm}$, and $r_0 = 2\,\text{mm}$. To keep things simple, we use two identical mechanical mirrors (MRs) with masses $m_1 = m_2 = 145\,\text{ng}$ each. They vibrate at around an oscillation frequency $\omega_1 = \omega_2 = 2\pi \times 947\,\text{kHz}$ and decay rates $\gamma_1(\gamma_2) = 140\,\text{kHz}$. The cavity where decay rates is $\kappa = 2\pi \times 215\,\text{kHz}$. We figure out the light's frequency using its speed and the wavelength of the light, which is 1064 nm. We pick some numbers for calculations, and the pump light's power is 9 mW. Since the mechanical part's frequency is higher than the light's fading speed, everything happens in a certain way.

4.1 Intra-Cavity Photon Number

The particles of light, that are present within a confined space called a cavity. This cavity is typically designed to trap and contain light. The concept is important in various fields like quantum optics and laser physics. The photon number within the cavity can vary based on factors such as the input of light, the characteristics of the cavity, and interactions with surrounding materials. Researchers often study the behavior of intra-cavity photon numbers to understand how light behaves in confined environments and how it interacts with matter. By controlling and manipulating the intra-cavity photon number, scientists can achieve effects like optical amplification, lasing, and quantum entanglement. This concept finds applications in technologies ranging from lasers and optical communication systems to quantum computing and precision measurement devices.

We're looking at how the number of steady photons changes when we change the laser power $\wp_l$,. There are specific points on the graph: critical points are where the curve has lower and higher stable sections, and inflection points P and Q show where the curve becomes unstable. When we start with a weak laser and slowly make it stronger, the photon intensity first follows the lower stable part S_1 of the curve, and then suddenly jumps to the upper stable part S_2 when the laser power reaches a certain value. if the driving laser

power are increase to 7.6mW. The upper stable part extends until a specific point. There's a dashed blue line that's unstable and goes between points P and Q. The unstable line slopes downward, but we can't really see it in real experiments. If we start with a strong laser and gradually weaken it, the photon number first follows the upper stable part, then jumps to the lower stable part at a different critical points x_{c+}, x_{c-}, and continues to decrease from there.

We present a comprehensive examination of controllable bistability, predominantly affected by factors like coupling frequencies and external modulation field strength. The intracavity photon count vs. laser power shows an S-shaped bistability curve at different levels of optomechanical coupling, with overlapping bifurcation curves for various coupling frequencies. Increasing optomechanical coupling strength G_0 enhances mechanical back-action, augmenting radiation pressure force and leading to photon dispersion within the cavity.

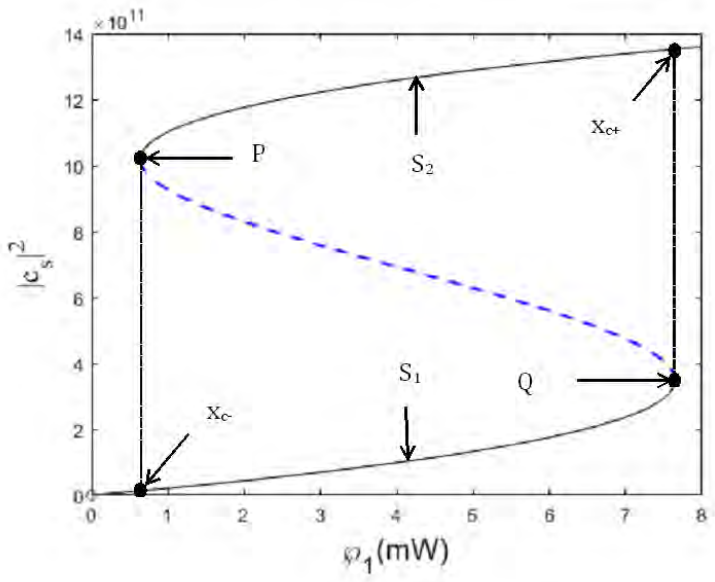

Figure 4.1: The average intracavity photon number $|C_s|^2$, in relation to the driving laser power, $\wp_l$,. These results are obtained using specific system parameters for this scenario, including $m_1 = m_2 = 145$ ng and $\omega_1 = \omega_2 = 947$ kHz, $\epsilon = \epsilon = 0$, and $G_0 = 2\pi \times 215$ kHz.

The bifurcation curve initially traces the upper stable branch at a lower cou-

pling regime, specifically at $G_0/2\pi = 6kHz$ (depicted by the solid black line). As the optomechanical coupling frequency is further increased, the upper stable path follows the lower stable path. This transition occurs at $G_0/2\pi = 7kHz$ (represented by the dashed black curve). Alongside the alteration in photon counts, enhancing the optomechanical coupling frequency also narrows the bistable curve. When G0, the optomechanical coupling strength G_0, is raised, the third lower stable path succeeds the second lower stable path, and vice versa.

4.2 Effect of external mechanical driving fields on optical bistability

The steady-state photon number's bistable curve without any external mechanical driving forces is represented as ϵ_1 and ϵ_2. We introduce external mechanical pumps to activate micro-resonators MR_1 and MR_2, investigating the sudden alterations in system bistability. Consequently, we apply mechanical pumps (acoustic stimulants) $\epsilon_j = \epsilon_j e^{-i\phi_1}$ (j = 1; 2) to the mechanical resonators MRs, analyzing their impact on the intracavity photon count, denoted as $|C_s|^2$.

Applying a mechanical pump field to MR_1 results in intriguing phase-sensitive optical phenomena in the NEOMS. By maintaining the constant amplitude ϵ and varying the phase angle ϕ, altering the angle from $\pi/4$ to π leads to amplified steady-state intracavity photon intensity,

An intriguing observation appears in the bistability plot, where the curves intersect at the same point and the upper stable branches follow one another, as do the lower stable paths. Conversely, when driving the second mechanical resonator MR_2, maintaining the constant amplitude ϵ_2 and altering the phase angle brings forth slight modifications in the upper stable branch of the curve. The transition between paths is evident as the blue solid, blue dashed, and black long-dashed curves shift.

Interestingly, this transition doesn't mirror in the lower stable paths, which remain independent of the phase angle. This behavior is attributed to the fact that the external modulating field only alters the effective Coulomb coupling

strength between the mirrors, without directly affecting the radiation pressure force.

By selectively driving mechanical resonators MR_1 and MR_2 while maintaining constant phase angles and varying amplitude, similar behaviors of the bistable curve can be observed. This demonstrates the complex interplay between external modulation, phase angles, and amplitude in shaping the optical responses of the system.

Chapter 5

Conclusion

We introduce a robust method for practically realizing optical switches using a nano-electro-opto-mechanical system (NEOMS). This complex setup comprises an optical resonator and two interconnected moving mirrors influenced by the electrostatic Coulomb force. Our study reveals optical and mirror bistability patterns, shaped by input laser power, coupling frequencies, and external mechanical influences on the mirrors. We explore the system's resilience and dynamic control by manipulating the mirrors' mechanical motion to influence the optical cavity field, and vice versa. By adjusting parameters like amplitude and phase angle, we selectively drive the mechanical resonators. We investigate optical bistability under varying conditions, including optomechanical and Coulomb coupling frequencies, and cavity detuning. Our findings demonstrate the controllable manipulation of steady-state photon bistability through input laser power adjustments. Furthermore, we report successful control of optical bistability using external mechanical driving fields on the mirrors. This control is achieved by selectively driving one of the mechanical pumps, enhancing the steady-state photon count and improving mirror motion. The amplitude and phase adjustments of external mechanical inputs influence the phase-sensitive bistability of static photon counts. Our study also uncovers mirror bistability influenced by optomechanical and Coulomb coupling strengths. Stable branches of bistable curves overlap at different mirror field coupling frequencies. The introduction of external mechanical driving fields results in the suppression and enhancement of mirror displacement

bistability. The combination of coupling frequency, switchable mechanical driving fields, cavity field detuning, and threshold laser power enables the development of adjustable optical switches and all-optical transistors. This work lays the foundation for potential extensions, including the achievement of multistable behaviors in both static photon intensity and mirror displacement.

Bibliography

[1] JS Al-Khalili, JA Tostevin, and IJ Thompson. Radii of halo nuclei from cross section measurements. *Physical review C*, 54(4):1843, 1996.

[2] Sohail Ahmed, Asma Javaid, Hui Jing, and Farhan Saif. Engineering optical and mirror bi-stability mechanically. *arXiv preprint arXiv:2307.05723*, 2023.

[3] Abid Ali, Farhan Saif, and Hiroki Saito. Phase separation and multistability of a two-component bose-einstein condensate in an optical cavity. *Physical Review A*, 105(6):063318, 2022.

[4] A Dorsel, John D McCullen, Pierre Meystre, E Vignes, and H Walther. Optical bistability and mirror confinement induced by radiation pressure. *Physical Review Letters*, 51(17):1550, 1983.

[5] Pierre Meystre, EM Wright, JD McCullen, and E Vignes. Theory of radiation-pressure-driven interferometers. *JOSA B*, 2(11):1830–1840, 1985.

[6] Human Microbiome Project Consortium. Structure, function and diversity of the healthy human microbiome. *Nature*, 486(7402):207–214, 2012.

[7] M Pinard, C Fabre, S Bourzeix, A Heidmann, E Giacobino, and S Reynaud. Quantum noise reduction using a cavity with a movable mirror. In *European Quantum Electronics Conference*, page QWD1. Optica Publishing Group, 1994.

[8] David Vitali, Paolo Tombesi, MJ Woolley, AC Doherty, and GJ Milburn. Entangling a nanomechanical resonator and a superconducting microwave cavity. *Physical Review A*, 76(4):042336, 2007.

[9] Claudiu Genes, A Mari, P Tombesi, and D Vitali. Robust entanglement of a micromechanical resonator with output optical fields. *Physical Review A*, 78(3):032316, 2008.

[10] M Abdi, Sh Barzanjeh, P Tombesi, and D Vitali. Effect of phase noise on the generation of stationary entanglement in cavity optomechanics. *Physical Review A*, 84(3):032325, 2011.

[11] Alexander Carmele, Berit Vogell, Kai Stannigel, and Peter Zoller. Optonanomechanics strongly coupled to a rydberg superatom: coherent versus incoherent dynamics. *New Journal of Physics*, 16(6):063042, 2014.

[12] Benjamin Rogers, N Lo Gullo, Gabriele De Chiara, G Massimo Palma, and Mauro Paternostro. Hybrid optomechanics for quantum technologies. *Quantum Measurements and Quantum Metrology*, 2(1):000010247820140002, 2014.

[13] F Bariani, S Singh, LF Buchmann, M Vengalattore, and P Meystre. Hybrid optomechanical cooling by atomic λ systems. *Physical Review A*, 90(3):033838, 2014.

[14] AH Safavi-Naeini, TP Mayer, J Chan, and M Eichen. eld, m. winger, q. lin, jt hill, de chang and o. painter. *Nature*, 472:69–73, 2011.

[15] T Rocheleau, T Ndukum, C Macklin, and JB Hertzberg. Aa clerk, and kc schwab. *Nature*, 463:72, 2010.

[16] Keith C Schwab and Michael L Roukes. Putting mechanics into quantum mechanics. *Physics Today*, 58(7):36–42, 2005.

[17] SA McGee, D Meiser, CA Regal, KW Lehnert, and MJ Holland. Mechanical resonators for storage and transfer of electrical and optical quantum states. *Physical Review A*, 87(5):053818, 2013.

[18] Muhammad Javed Akram and Farhan Saif. Complex dynamics of nanomechanical membrane in cavity optomechanics. *Nonlinear Dynamics*, 83:963–970, 2016.

[19] JM Fink, M Göppl, M Baur, R Bianchetti, Peter J Leek, Alexandre Blais, and Andreas Wallraff. Climbing the jaynes–cummings ladder and observing its nonlinearity in a cavity qed system. *Nature*, 454(7202):315–318, 2008.

[20] Lin Tian. Optoelectromechanical transducer: Reversible conversion between microwave and optical photons. *Annalen der Physik*, 527(1-2):1–14, 2015.

[21] Lin Tian and Peter Zoller. Coupled ion-nanomechanical systems. *Physical review letters*, 93(26):266403, 2004.

[22] Steven D Bennett, Jesse Maassen, and Aashish A Clerk. Scattering approach to backaction in coherent nanoelectromechanical systems. *Physical review letters*, 105(21):217206, 2010.

[23] David J Wineland, Christopher Monroe, Wayne M Itano, Dietrich Leibfried, Brian E King, and Dawn M Meekhof. Experimental issues in coherent quantum-state manipulation of trapped atomic ions. *Journal of research of the National Institute of Standards and Technology*, 103(3):259, 1998.

[24] A Szöke, V Daneu, J Goldhar, and NA Kurnit. Bistable optical element and its applications. *Applied Physics Letters*, 15(11):376–379, 1969.

[25] Kashif Ammar Yasir and Wu-Ming Liu. Tunable bistability in hybrid bose-einstein condensate optomechanics. *Scientific reports*, 5(1):10612, 2015.

[26] A Dalafi, MH Naderi, M Soltanolkotabi, and Sh Barzanjeh. Controllability of optical bistability, cooling and entanglement in hybrid cavity optomechanical systems by nonlinear atom–atom interaction. *Journal of Physics B: Atomic, Molecular and Optical Physics*, 46(23):235502, 2013.

[27] Qing Sun, Xing-Hua Hu, WM Liu, XC Xie, and An-Chun Ji. Effect on cavity optomechanics of the interaction between a cavity field and a one-dimensional interacting bosonic gas. *Physical Review A*, 84(2):023822, 2011.

[28] Suzhen Zhang, Jiahua Li, Rong Yu, Wei Wang, and Ying Wu. Optical multistability and fano line-shape control via mode coupling in whispering-gallery-mode microresonator optomechanics. *Scientific Reports*, 7(1):39781, 2017.

[29] Kamran Ullah. Electro-optomechanical switch via tunable bistability and four-wave mixing. *Chinese Physics B*, 28(11):114209, 2019.

[30] Hyatt Gibbs. *Optical bistability: controlling light with light*. Elsevier, 2012.

[31] Shum Ping, Lu Chao, et al. Bistability threshold inside hysteresis loop of nonlinear fiber bragg gratings. *Optics Express*, 13(13):5127–5135, 2005.

[32] APH Gonzalez-Marcos, A Hurtado, and J Antonio Martin-Pereda. Optical bistable devices as sensing elements. In *Unmanned/Unattended Sensors and Sensor Networks*, volume 5611, pages 63–70. SPIE, 2004.

[33] Steven D Bennett, Lynda Cockins, Yoichi Miyahara, Peter Grütter, and Aashish A Clerk. Strong electromechanical coupling of an atomic force microscope cantilever to a quantum dot. *Physical review letters*, 104(1):017203, 2010.

[34] Kwan H Lee, Terry G McRae, Glen I Harris, Joachim Knittel, and Warwick P Bowen. Cooling and control of a cavity optoelectromechanical system. *Physical Review Letters*, 104(12):123604, 2010.

[35] Ying-Dan Wang and Aashish A Clerk. Using dark modes for high-fidelity optomechanical quantum state transfer. *New Journal of Physics*, 14(10):105010, 2012.

[36] Colm Ryan, Hanhee Paik, and Raytheon BBN Technologies Corp. Cambridge United States. " superconducting qubit optical transducer"(sqot). Technical report, 2015.

[37] Terry G McRae, Kwan H Lee, Glen I Harris, Joachim Knittel, and Warwick P Bowen. Cavity optoelectromechanical system combining strong electrical actuation with ultrasensitive transduction. *Physical Review A*, 82(2):023825, 2010.

[38] Qiang Lin, Jessie Rosenberg, Darrick Chang, Ryan Camacho, Matt Eichenfield, Kerry J Vahala, and Oskar Painter. Coherent mixing of mechanical excitations in nano-optomechanical structures. *Nature Photonics*, 4(4):236–242, 2010.

[39] Francesco Massel, Sung Un Cho, Juha-Matti Pirkkalainen, Pertti J Hakonen, Tero T Heikkilä, and Mika A Sillanpää. Multimode circuit optomechanics near the quantum limit. *Nature communications*, 3(1):987, 2012.

[40] Arne Barfuss, Jean Teissier, Elke Neu, Andreas Nunnenkamp, and Patrick Maletinsky. Strong mechanical driving of a single electron spin. *Nature Physics*, 11(10):820–824, 2015.

[41] Inah Yeo, Pierre-Louis de Assis, Arnaud Gloppe, Eva Dupont-Ferrier, Pierre Verlot, Nitin S Malik, Emmanuel Dupuy, Julien Claudon, Jean-Michel Gérard, Alexia Auffèves, et al. Strain-mediated coupling in a quantum dot–mechanical oscillator hybrid system. *Nature nanotechnology*, 9(2):106–110, 2014.

[42] AA Clerk, X Waintal, and PW Brouwer. Fano resonances as a probe of phase coherence in quantum dots. *Physical review letters*, 86(20):4636, 2001.

[43] M Vengalattore, M Hafezi, MD Lukin, and M Prentiss. Optical bistability at low light level due to collective atomic recoil. *Physical review letters*, 101(6):063901, 2008.

[44] Ferdinand Brennecke, Stephan Ritter, Tobias Donner, and Tilman Esslinger. Cavity optomechanics with a bose-einstein condensate. *Science*, 322(5899):235–238, 2008.

[45] Tom P Purdy, DWC Brooks, Thierry Botter, Nathan Brahms, Z-Y Ma, and Dan M Stamper-Kurn. Tunable cavity optomechanics with ultracold atoms. *Physical review letters*, 105(13):133602, 2010.

[46] Roohollah Ghobadi, AR Bahrampour, and C Simon. Quantum optomechanics in the bistable regime. *Physical Review A*, 84(3):033846, 2011.

[47] Eyob A Sete, H Eleuch, and Sumanta Das. Semiconductor cavity qed with squeezed light: Nonlinear regime. *Physical Review A*, 84(5):053817, 2011.

[48] Cheng Jiang, Hongxiang Liu, Yuanshun Cui, Xiaowei Li, Guibin Chen, and Xuemin Shuai. Controllable optical bistability based on photons and phonons in a two-mode optomechanical system. *Physical Review A*, 88(5):055801, 2013.

[49] Nan Xu, Ze-Di Cheng, Jin-Dao Tang, Xiao-Min Lv, Tong Li, Meng-Lin Guo, You Wang, Hai-Zhi Song, Qiang Zhou, and Guang-Wei Deng. Recent advances in nano-opto-electro-mechanical systems. *Nanophotonics*, 10(9):2265–2281, 2021.

[50] Tian-Xiang Lu, Ya-Feng Jiao, Hui-Lai Zhang, Farhan Saif, and Hui Jing. Selective and switchable optical amplification with mechanical driven oscillators. *Phys. Rev. A*, 100:013813, Jul 2019.

[51] Sebastian G Hofer and Klemens Hammerer. Quantum control of optomechanical systems. In *Advances in Atomic, Molecular, and Optical Physics*, volume 66, pages 263–374. Elsevier, 2017.

[52] Michel Pinard, Y Hadjar, and Antoine Heidmann. Effective mass in quantum effects of radiation pressure. *The European Physical Journal D-Atomic, Molecular, Optical and Plasma Physics*, 7:107–116, 1999.

[53] DF Walls and Gerard J Milburn. Bose-einstein condensation. In *Quantum Optics*, pages 397–420. Springer, 2008.